Proceedings of the XVII ECSMGE-2019
Geotechnical Engineering foundation of the future
ISBN 978-9935-9436-1-3

doi: 10.32075/17ECSMGE-2019-0236

XVII European Conference
ECSMGE 2019
Reykjavik
on Soil Mechanics
and Geotechnical Engineering

Load redistribution of piles affected by tunnelling: hybrid centrifuge tests using fibre Bragg grating

Redistribution de la charge des pieux affectés par le tunnelage: essais de centrifugation hybride utilisant des fibres optiques à réseau de Bragg

Song. G., Marshall, A.M., and Heron, C.M.
University of Nottingham, Nottingham, UK

ABSTRACT: The construction of tunnels close to existing piles may affect the load carrying capacity of the piles. The severity of these effects is related to the proximity of the pile to the tunnel, as well as how the pile mobilises its capacity (i.e. along its shaft or at its base). To further understand the effect of tunnelling on piles, it is essential to consider how the load is redistributed along/or between the piles during tunnelling. This paper presents experimental data from hybrid geotechnical centrifuge tests that simulate tunnelling induced ground movement and its effect on piles in dry sand. The hybrid tests model the tunnel and piles within the centrifuge and share data in real-time with a numerical model which simulates the superstructure, thereby achieving an accurate simulation of the global tunnel-soil-pile-structure interaction problem. A fibre Bragg grating (FBG) sensor system was used to measure the distribution of strain along the piles, allowing assessment of the pile load distribution during tunnel volume loss.

RÉSUMÉ: La construction de tunnels à proximité de pieux existants peut affecter la capacité de charge des pieux. L'importance de ces effets est liée à la proximité du pieu par rapport au tunnel, ainsi qu'à la façon dont le pieu mobilise sa capacité (c'est-à-dire le long de son puits ou à sa base). Pour mieux comprendre l'effet des tunnels sur les pieux, il est essentiel d'examiner la manière dont la charge est redistribuée le long des pieux / ou entre les pieux lors de la construction des tunnels. Cet article présente des données expérimentales d'essais centrifuge géotechniques hybrides simulant le mouvement du sol induit par les tunnels et son effet sur les pieux dans le sable sec. Les tests hybrides modélisent le tunnel et les pieux dans la centrifugeuse et partagent les données en temps réel avec un modèle numérique simulant la superstructure, réalisant ainsi une simulation précise du problème de l'interaction global tunnel-sol-pieu-structure. Un système de fibres optiques à réseau de Bragg (FBG) a été utilisé pour mesurer la distribution de la contrainte le long des pieux, permettant d'évaluer la distribution de la charge du pieu lors de la perte de volume du tunnel.

Keywords: Tunnel; pile; fiber Bragg grating

1 INTRODUCTION

There is considerable demand for underground construction such as tunnelling to reduce overground congestion in developed urban areas. Tunnel construction inevitably results in soil disturbance that could cause damage to nearby structures, such as piled buildings. Centrifuge testing has been widely used as a tool to investigate tunnel-pile-structure-interaction (TPSI) problems (Loganathan et al. 2000; Jacobsz et al. 2004; Chiang and Lee 2007; Marshall and Mair 2011; Ng et al. 2014; Franza and Marshall 2017). Physical simulation of piled

structures is generally simplified using constant load isolated piles or pile groups, or by using an equivalent beam/plate to represent a building (i.e. piles are rigidly connected to a plate). The use of simplified models could over- or under-predict the contribution of superstructure effects to the global TPSI problems. As a result, accurately simulating the superstructure is vital for the study of TPSI. This paper provides results from tests using coupled centrifuge-numerical modelling (CCNM) (Franza and Marshall 2018), a hybrid test method combining physical and numerical modelling in order to achieve an accurate simulation of the TPSI problem. The superstructure is simulated in the numerical model, the soil and piles are simulated in the physical model, and data is shared at the pile-superstructure interface (the shared boundary) using a real-time coupling control system (Idinyang et al. 2018). In the tests presented here, fibre Bragg grating was used to measure model pile strains. Fibre Bragg grating has certain advantages in relation to conventional strain gauges, including less space requirements on the model pile and insensitivity to electrical noise. In this paper, results from three centrifuge tests are presented to illustrate the effects of superstructure stiffness on piles load redistribution due to tunnelling induced ground movements. A modified CCNM system was developed, combined with the use of FBGs within the centrifuge environment.

2 EXPERIMENTAL SYSTEM & SET UP

Centrifuge tests were conducted on the University of Nottingham Centre for Geomechanics (NCG) 2 m radius, 50 g-tonne geotechnical centrifuge at an acceleration of 80 times gravity (i.e. 80 g). Figure 1 shows the layout of the testing geometry and configuration. Three centrifuge tests were conducted, which are: (1) pile loading test (PL), (2) constant load pile group test (CL) and (3) pile group with the consideration of structure stiffness (CCNM2). The centrifuge strong box used for testing was 150 mm wide, 700 mm long, and 400 mm high (internal dimensions). The model tunnel had a diameter of 90 mm and was located 75 mm above the strongbox base. Leighton Buzzard Fraction E sand with a D_{50} of 0.12 mm was used for the tests. The sand has a specific gravity G_S of 2.65. The maximum (e_{max}) and minimum (e_{min}) void ratios of the sand are 1.01 and 0.61, respectively.

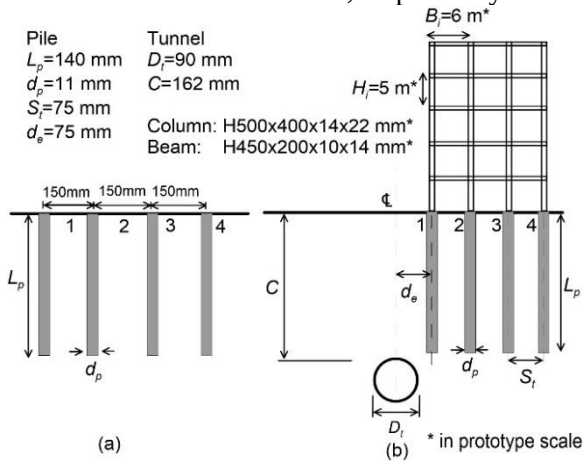

Figure 1 Test layout: (a) pile loading test, and (b) tunnelling beneath piled frame (model scale)

2.1 Centrifuge model

The centrifuge model is shown in Figure 2. Tunnel volume loss was simulated using a rigid boundary eccentric mechanical model tunnel (Song et al., 2018), which provides non-uniform radial displacements around the tunnel lining, causing maximum soil displacements at the tunnel crown and no displacements at the tunnel invert. The modified CCNM system (originally developed by Franza and Marshall, 2018), also presented in Figure 2, allows individual control of each model pile using a single linear actuator. The control system enables either force or displacement control of the piles. The modular actuator system allows for easy adaptation of its configuration. Each model pile is connected to an actuator via a loading shaft with a 5 kN in-line load cell.

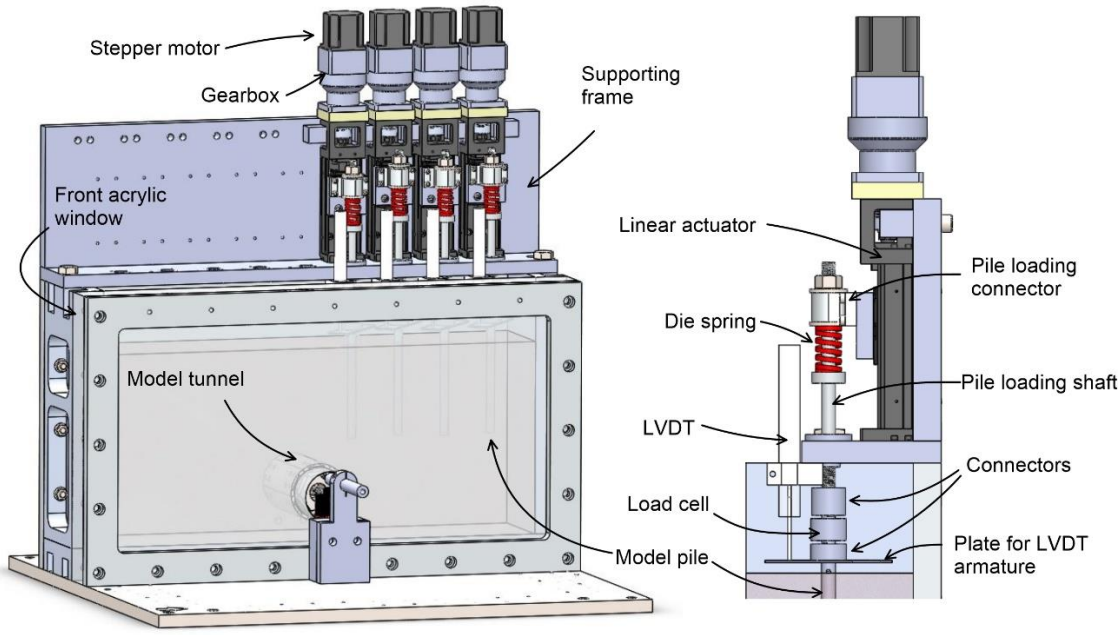

Figure 2 Centrifuge model layout

A die spring (stiffness rate of 219 N/mm) is required between the driving actuator to reduce the sensitivity of the load response to movements of the actuator, which was necessary to ensure the control system remained stable (Franza and Marshall, 2018). Linear variable differential transformers (LVDTs) are located at the base of the supporting frame with their armatures resting on a plate fixed to the pile head. The linear actuators have a maximum stroke distance of 40 mm with a 5 kN capacity. The model piles were made from 10 mm diameter cylindrical aluminium rod. A rough soil-pile interface was created by bonding sand to the piles, resulting in a final pile diameter of d_p=11 mm, and an axial stiffness of the piles at prototype scale of EA=11 GN/m (within the expected range of full-scale 0.9 m diameter concrete piles). The aluminium model piles were instrumented with FBGs inside the pile, which was beneficial compared to the use of conventional strain gauges which, due to space/installation issues, could only have been placed on the outer surface of the pile, thereby affecting the outer interface. Further details of the FBG instrumentation method and application are provided in a subsequent section.

2.2 Numerical model

The numerical model was developed using ABAQUS (Hibbitt et al. 2001) and simulated a five-storey steel frame building designed for storage and machine plant use. Building elements such as stairways, façade, and bracings were not considered for the structural stiffness calculation. A linear elastic constitutive model was used for the steel frame with Young's modulus $E = 2.1 \times 10^{11}$ N/m^2 in prototype scale and Poisson's ratio μ=0.3. The dimensions of the steel frame building, including column and beam size, are given in Figure 1 (prototype scale). The variable load applied to the building is based on the Eurocode specifications (Gulvanessian et al. 2009) for storage building (7.5 kN/m^2) and the permanent load is 3 kN/m^2, which gives a total load of 2364 kN for the two inner piles and 1630 kN for the two outer piles (prototype scale).

2.3 Sample preparation

The model was prepared at 1 g using dry air sand pluviation. To achieve a consistent soil density around the model tunnel, the front acrylic window was placed facing downwards, and the model tunnel was placed into position, allowing sand to be poured around the tunnel. As a result, the sand dropping direction is in line with the tunnel axis; this method is consistent with various other centrifuge tests (Jacobsz et al. 2004; Marshall and Mair, 2011). The sand pouring rate and drop height were calibrated to obtain a relative density of approximately 90%. After sand pouring, the back plate was secured and the box carefully rotated to its upright position. To replicate non-displacement piles, the piles were then pushed at 1 g into the sand, starting with the pile closest to the tunnel and moving outwards, using the support frame to ensure the pile were vertical. The linear actuator was then connected to the pile head and the tunnel volume loss control system (gearbox and stepper motor) and LVDTs installed.

2.4 Instrumentation

Fibre Bragg grating (FBG) sensors were used to measure the axial force distribution along the piles. The sensors were made from a single mode optical fibre. Each fibre contains three FBGs written using an excimer laser (reflectivity of 90%) with a centre wavelength of 1530, 1535, and 1540 nm or 1545, 1550, 1560 nm. Each pile contains two fibres located on the opposite inner face of the pile. A four-channel commercial FBG interrogator (CASSTK) capable of scanning wavelengths of 1525-1565 nm at a frequency of 2 Hz was used to measure the FBG wavelength shifts. The FBG interrogator was mounted in the centrifuge cabinet and was exposed to g-levels of 4-7 *g* during tests. For each pile consisting of two fibres, a splitter (coupler) was used, which gives an even split ratio from one input fibre (regardless of input wavelength) to two output fibres; a detailed configuration is shown in Figure 3. To enable temperature compensation, one additional FBG was located at the pile head (pile 2 only).

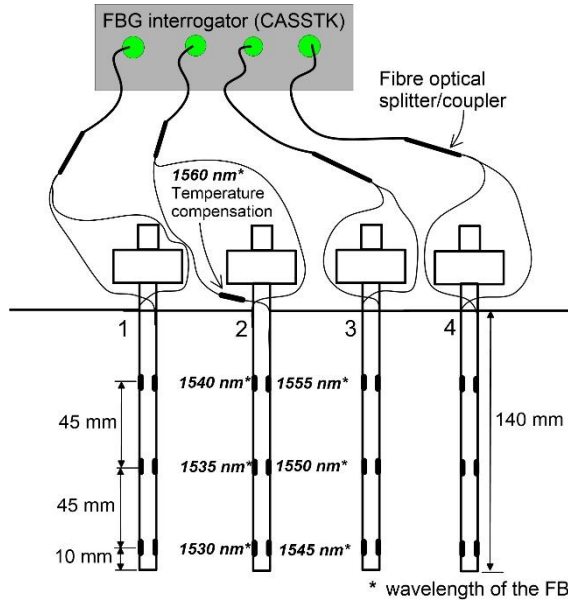

Figure 3 Test setup for FBGs and Interrogator

2.5 Test procedure

A constant 5 N vertical load was maintained at the pile head (load controlled) during centrifuge spin-up to 80 g. This was done to ensure minimum relative displacement occurred between the soil and pile during spin-up (if fixed in place during spin-up, the soil would settle more than the pile). Three stabilisation cycles (going from 80 g to 10 g and back to 80 g) were performed to encourage a uniform stress distribution within the soil body and improve repeatability between tests. The piles were then loaded to the designated working load (255 N for outer piles 1 and 4, and 370 N for inner piles 2 and 3; refer to pile numbering in Figure 1) in 50 N stages, starting with pile 1 and moving sequentially to pile 4. For test CL (structure with zero stiffness), these initial pile loads were maintained throughout the volume loss process. For test CCNM2 (structure with stiffness), the real-time interface was activated, followed by the initiation of ABAQUS (simulating the steel frame structure). This final step gives control of

the pile loads in the centrifuge to the ABAQUS program, which takes in measurements of pile displacements from the centrifuge and outputs new pile loads based on the outcomes of the structural numerical simulation; the pile loads are then passed back to the control system, and the load on the piles is adjusted accordingly. The tunnel volume loss ($V_{l,t}$) process is then started, increasing up to 3% in increments of approximately 0.1%.

3 RESULTS

3.1 Pile load capacity

The pile load capacity was determined by in-flight pile driving tests on all four piles (Test PL) in the following order of pile number: 2-4-3-1 (no model tunnel was included). Displacement control was used during pile driving, with an actuator rate of 0.1 mm/s. Note that this is the speed of the actuator; the rate of pile displacement varies somewhat during driving due to the effect of the die spring. Figure 4 presents the load versus pile settlement (S_d) normalised by pile diameter (d_p) curve for pile 2, including data from the load cell and three FBG sensors along the pile (labelled S1, S2, etc). The offset of the FBG data near the origin is due to a lower logging frequency in the FBG analyser (1 Hz) compared to the load/displacement data acquisition system. The assumption was made that the ultimate load capacity of the non-displacement piles is defined at the point when the pile shaft resistance is fully mobilised. The accumulated shaft resistance (as a force) along the pile is shown in Figure 5, which demonstrates that shaft resistance was fully mobilised at S_d/d_p of about 8% (this was sufficiently consistent and conservative for all piles). This magnitude of settlement corresponds closely to the point where the rate of pile settlement increased. At S_d/d_p=8%, pile 2 capacity was 893 N, which was a conservative value for all piles. Considering the total load applied to the piles during the tunnel-pile interaction tests (255/370 N for outer/inner piles at model scale), this gives a factor of safety of 3.5 and 2.4 for outer and inner piles, respectively.

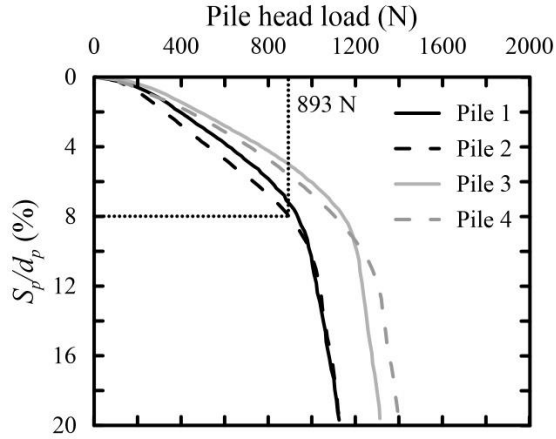

Figure 4 Load settlement curve for loading test: pile 2

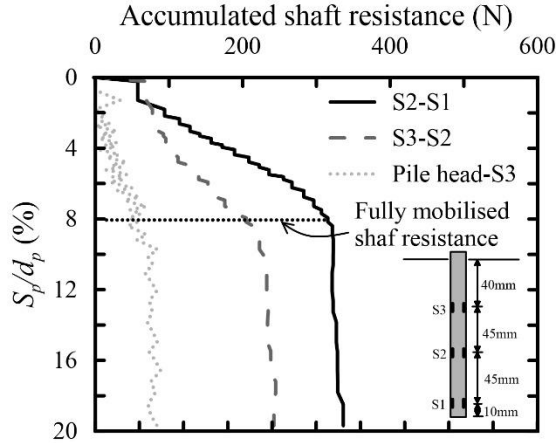

Figure 5 Shaft resistance during loading test: pile 2

3.2 Effect of structure stiffness on pile load transfer and settlement

Two centrifuge tests were conducted to study the effect of structure stiffness on pile load transfer and pile settlement due to tunnelling: CL (zero structure stiffness, equivalent to constant pile head load) and CCNM2 (structure stiffness simulated using the hybrid testing technique). Figure 6 shows the variation of pile head load (upper plots) and normalised pile head settlement (lower plots) as tunnel volume loss was increased up to 3%. For test CL, where pile head load is

constant, the piles settle differently according to their location. In test CCNM2, the pile loads vary during tunnel volume loss according to the characteristics of the structure modelled in ABAQUS. It can be seen that piles 1 and 4 experience a reduction in load, whereas loads increased in piles 2 and 3 (most significantly in pile 2; very little change is noted in pile 3). The lower plots show that these changes in pile head load during test CCNM2 did not have a significant impact on the settlements that occurred during tunnel volume loss compared to the constant-load CL test. The only marginal difference is for pile 2, which has a slightly higher settlement at $V_{l,t}$ = 3% in test CCNM2 due to the higher pile head load. The similarity between settlement results for CCNM2 and CL tests is due to the use of piles with relatively high safety factors; Franza and Marshall (2018) demonstrated that load redistribution caused by a superstructure on piles with relatively low safety factors of about 1.5 has a significant impact on their settlement response during tunnelling (for both displacement and non-displacement piles).

The load distribution along each pile is presented in the upper plots of Figure 7. The load applied to the pile head is carried by shaft friction force (Q_s) and end bearing force (Q_p). The end bearing force at the pile tip was not measured directly but can be inferred from the difference between pile head load and accumulated resistance along the pile shaft (also the lowest shaft measurement point was only 10 mm from the base, hence the load reading at that location gives a good approximation of the base load). The change in unit shaft friction along the pile depth during tunnel volume loss ($\Delta f_{vl}(z)$) can be calculated from the variation of axial force measured along the pile:

$$\Delta f_{vl}(z) = \frac{\Delta Q_s^f(z) - \Delta Q_s^i(z)}{\Delta z} \quad (1)$$

where superscripts *f* and *i* relate to data after and before tunnel volume loss, respectively, and Δz is the distance between the two measurement points. Figure 7 (lower plots) shows the change in unit shaft friction at a tunnel volume loss of $V_{l,t}$= 3%.

In test CL, pile 1 (Figure 7(a) upper plot) exhibits a reduction in shaft loads due to tunnel volume loss, with axial pile load going into negative values close to the pile tip at $V_{l,t}$=3%. To maintain the constant pile head load, Figure 7(a) (lower plot) shows that unit skin friction is increased along the upper portion of the pile (0-80mm below soil surface). A similar reduction in unit shaft resistance close to the pile tip is observed for test CCNM2, despite the reduction in pile head load due to the effect of structure stiffness. The trends and magnitudes of change of unit shaft resistance along the length of pile 1 caused by tunnel volume loss are similar between tests CCNM2 and CL, except for 40-80 mm, where the CCNM2 pile mobilised less resistance (which made up most of the difference between the applied head load at $V_{l,t}$=3%).

For pile 2, there is a small increase in axial force close to the pile tip for test CL at $V_{l,t}$=3% (assuming that the deepest shaft measurement point is mainly affected by the pile base resistance). In test CL, an increase in pile base resistance requires a reduction in shaft friction and hence a reduction of unit shaft friction is observed along the lower portions of the pile (Figure 7(b) lower plot). For test CCNM2, as the pile head load is increased, there is an evenly distributed increase in unit shaft resistance along the pile length. For pile 3, the axial force along the pile did not change significantly for both tests. Pile 4 head load decreased with tunnel volume loss in test CCNM2, with shaft loads decreasing mainly within the lower portions of the pile.

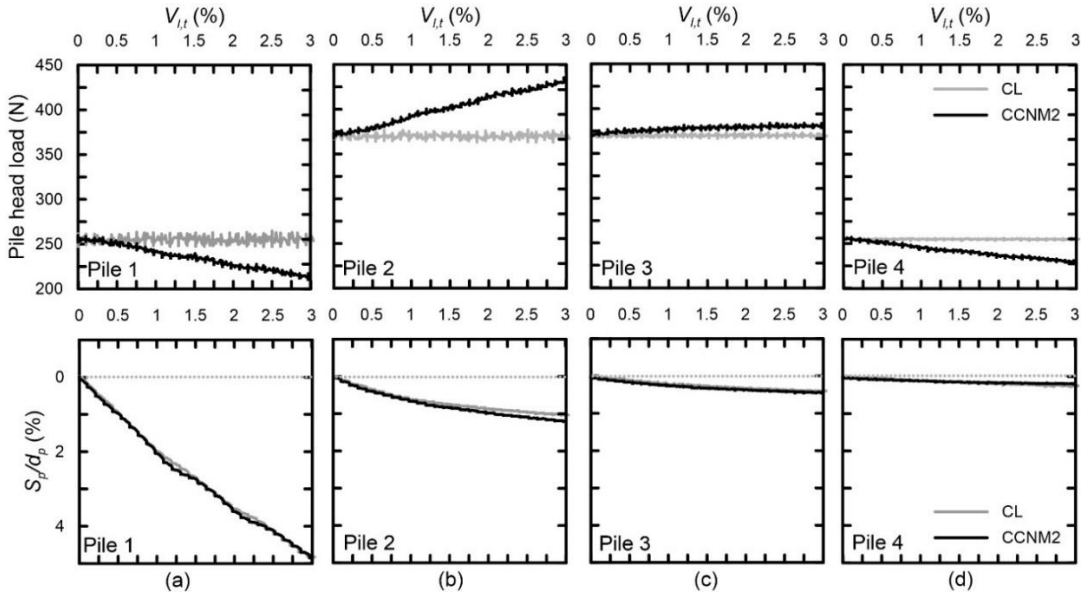

Figure 6 Pile settlement and head load with tunnel volume loss: (a) pile 1, (b) pile 2, (c) pile 3, (d) pile 4

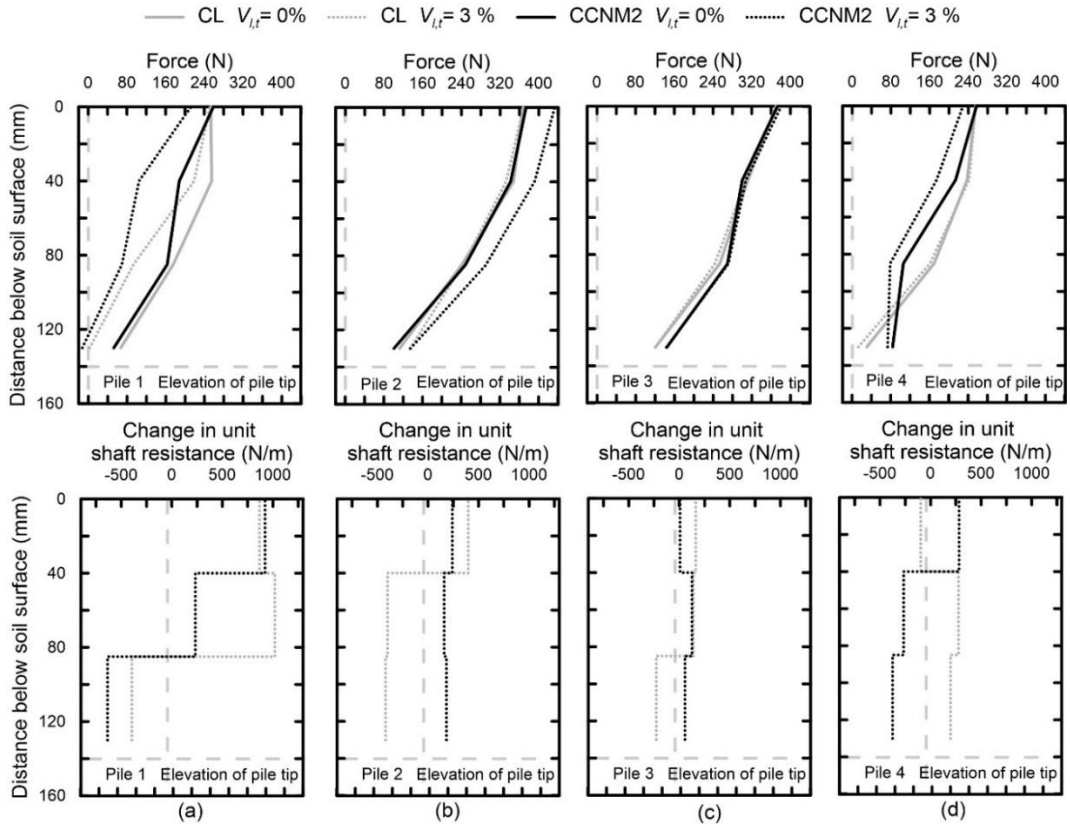

Figure 7 Pile axial load at $V_{l,t}$= 0% and 3% and change in unit shaft resistance at $V_{l,t}$= 3%: (a) pile 1, (b) pile 2, (c) pile3, (d) pile 4

4 CONCLUSIONS

This paper presented results from geotechnical centrifuge tests aimed at evaluating the effect of tunnelling on non-displacement piles in dry sand. A hybrid centrifuge testing technique (CCNM) was used which can replicate the realistic load redistribution among piles caused by a connected superstructure during tunnelling by coupling the centrifuge test with a numerical model that simulates the superstructure. A fibre Bragg grating system was used to measure pile strains and evaluate changes in pile load profiles during tunnelling. Pile loading tests indicated that shaft friction was fully mobilised at a normalised settlement of S_d/d_p = 8%, which was used to define the load capacity of the piles and initial pile safety factor (which varied from 2.5 to 3.6) for the tunnel-pile interaction tests. Compared to the tunnel-pile interaction test with constant pile head loads, the CCNM test which adjusted pile head loads during tunnel volume loss showed that the pile load closest to the tunnel dropped and that the load of the adjacent pile increased. The redistribution of loads as a result of the superstructure stiffness did not have a significant impact on pile head settlement, which could be expected for non-displacement piles with relatively high safety factors since the necessary resistance is quickly mobilised along the pile shafts.

5 REFERENCES

Lee, C. J., & Chiang, K. H. 2007. Response of single piles to tunneling-induced soil movements in sandy ground. *Canadian Geotechnical Journal*, **44**(10), 1224-1241.

Franza, A., & Marshall, A. M. 2017. Centrifuge modelling study of the response of piled structures to tunnelling. *Journal of Geotechnical and Geoenvironmental Engineering*, **144**(2), 04017109.

Franza, A., & Marshall A. M. 2018. Centrifuge and real-time hybrid testing of tunnelling beneath piles and piled buildings. *Journal of Geotechnical and Geoenvironmental Engineering* **145**(3), 04018110..

Gulvanessian, H., Formichi P., & Calgaro J.A. 2009. Designers' Guide to Eurocode 1: Actions on Buildings: EN1991-1-1. Thomas Telford Ltd.

Hibbitt, K,. & Sorensen 2001. ABAQUS/Explicit: User's Manual, Volume **1**. Karlsson and Sorenson Incorporated.

Idinyang, S., Franza, A., Heron, C. M., & Marshall, A. M. 2018. Real-time data coupling for hybrid testing in a geotechnical centrifuge. *International Journal of Physical Modelling in Geotechnics*, 10.1680/jphmg.17.00063.

Jacobsz, S. W., Standing, J. R., Mair, R. J., Hagiwara, T., and Sugiyama, T. (2004). Centrifuge modelling of tunnelling near driven piles. *Soils and Foundations*, **44**(1), 49–56.

Loganathan, N., Poulos H. G., & Stewart, D. P. 2000. Centrifuge model testing of tunnelling-induced ground and pile deformations. *Geotechnique* **50**(3), 283–294.

Marshall, A. M. & Mair, R. J. 2011. Tunnelling beneath driven or jacked end bearing piles in sand. *Canadian Geotechnical Journal* **48**(12), 1757–1771.

Ng, C. W. W., Soomro, M. A., & Hong Y. 2014. Three-dimensional centrifuge modelling of pile group responses to side-by-side twin tunnelling. *Tunnelling and underground space technology* **43**, 350–361.

Song, G., Marshall, A. M., & Heron C. M. 2018. A mechanical displacement control model tunnel for simulating eccentric ground loss in the centrifuge. *In Physical Modelling in Geotechnics, Volume 1: Proceedings of the 9th International Conference on Physical Modelling in Geotechnics (ICPMG2018)*, July 17-20, 2018, London, United Kingdom, pp. 455. CRC Press